Time transfer by laser link: a complete analysis of the uncertainty budget

Time transfer by laser link: a complete analysis of the uncertainty budget

E Samain[1], P Exertier[1], C Courde[1],P Fridelance[2], P Guillemot[3], M Laas-Bourez[1] and J-M Torre[1]

[1] GeoAzur—Observatoire de la Côte d'Azur, 2130 route de l'Observatoire, 06460 Caussols, France
[2] Phusipus Intégration, 8 Allée Bellevue, Saint Vallier de Thiey, France
[3] CNES—French Space Agency, 18 av Edouard Belin, 31400 Toulouse, France

E-mail: etienne.samain@oca.eu

CrossMark

Abstract

The Time Transfer by Laser Experiment (T2L2) on the Jason 2 satellite is a mission allowing remote clocks synchronization at the picosecond level. It is based on laser ranging technologies, with a laser station network on the ground and a dedicated instrument on board the satellite. It was launched in June 2008 and has been working continuously since then. T2L2 performances are very promising for time and frequency metrology and also for fundamental physics. The scientific objectives of the whole experiment rely on a rigorous uncertainty budget. This is governed by the characteristics of the space instrument and the laser stations network, the post treatment done on the ground, and also the process used to calibrate the laser stations. The uncertainty budget demonstrates that T2L2 is able to perform common-view time transfers between remote sites with an expanded uncertainty better than 140 ps (coverage factor = 2).

(Some figures may appear in colour only in the online journal)

1. Introduction

T2L2 [1–3] is a two-way time transfer mission based on the timing of optical pulses emitted by a network of laser stations and detected by a dedicated space instrument. It allows for the synchronization of remote clocks with a time stability in the range of a few picoseconds over hundreds of seconds. After four unsuccessful proposals, in 2005 T2L2 was accepted as a passenger instrument on the Jason 2 altimetry satellite. It was launched in June 2008 and has been working without any major interruption since that time. It was put in place by a Delta launcher at an altitude of 1336 km and an inclination of 66°.

The elementary T2L2 link is a ground-space time transfer between a given laser station and the space instrument. For a time comparison between two laser stations, several ground

to space elementary links are used for each ground station. To realize the ground-space transfer, the laser station emits asynchronous short light pulses towards the satellite. A reflector array on board the satellite returns some of the light pulses to the ground station. The epoch of the laser emission t_E and the epoch of the reception t_R are measured according to the ground station's timescale. The T2L2 payload records the arrival time t_B of laser pulses according to the timescale of the space clock. Schematically, the time offset Δ_{AS} between a ground clock A and the space clock S is computed for each laser pulse, where the difference between the start and the arrival epochs is shifted by the time of flight divided by two. Δ_{AS} is given by:

$$\Delta_{AS} = t_E + \frac{t_R - t_E}{2} - t_B + C_{AS} \qquad (1)$$

where C_{AS} is a correction term that takes into account instrumental calibrations, atmospheric phenomena, speed aberrations and relativistic effects. The T2L2 data are very interesting for both time and frequency metrology and for fundamental
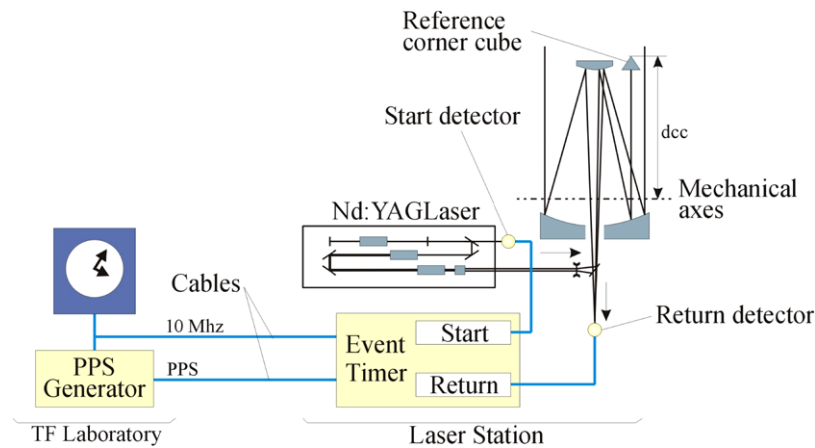
Figure 1. Simplified scheme of a typical laser station. Time and frequency equipments are generally located in a dedicated laboratory.

physics. For instance, T2L2 is able to calibrate and validate the best available microwave time transfer techniques [4, 5] and will be able to compare the time transfer systems embedded on the new mission ACES (Atomic Clock Ensemble in Space) that will be launched on the ISS (International Space Station) in 2017 [6]. The possibilities given by an accurate time transfer between remote clocks is also of interest for the search for a potential anisotropy of the speed of light [7] or for the validation of one-way laser ranging for some future tests involving solar orbit [8, 9]. All these scientific objectives rely on a rigorous uncertainty budget for the whole experiment that is governed by the characteristics of both the space instrument and the laser stations network, as well as the calibration process used on the ground.

In section 2 we give a brief description of the whole instrumentation (ground and space) involved in a T2L2 time transfer. In sections 3 and 4, we describe the time transfer equations for both the ground to space and the ground to ground links. Then, from these equations, we give in section 5 the uncertainty budget of a typical T2L2 time transfer.

2. Instrumentation

The ground-level part of the T2L2 time transfer is based on the international laser station network [10]. This gathers data from more than 40 laser ranging stations over the world and is driven by the International Laser Ranging Service (ILRS) which provides global satellite and lunar laser ranging data to support research in many scientific domains such as geodesy, geophysics, lunar science, and fundamental physics.

A typical laser station is composed of the following elements (figure 1):

- A clock to give the station a frequency reference (5 or 10 MHz). From this frequency reference a numerical divider generates a one pulse per second signal (PPS) for timescale purposes. For laser ranging, this clock is used to measure the time interval between the start and the return; for T2L2, it is the clock which has to be synchronized.
- A neodymium YAG doubled laser to generate pulses at a rate of between 10 Hz and 2 kHz. The wavelength is

usually 532 nm and the full width at half maximum is between 50 ps to 200 ps.
- A telescope to transmit and receive laser pulses. Some stations have the same telescope for both transmission and reception, while others have two distinct apertures.
- A start detector to generate the start reference at the output of the laser.
- A return detector to detect pulses which have been reflected by the satellite.
- An event timer that has two independent channels to time tag the electrical pulses of both start t_E and return t_R detectors. The time setting of the event timer is carried out at the first initialization with the PPS signal delivered by the clock of the time and frequency standard laboratory.

The T2L2 space equipment is an instrument able to time with picosecond resolution the arrival of all laser pulses arriving from the laser stations. It comprises a photo-detection device and an event timer. This equipment is associated with an ultra-stable quartz oscillator used as the T2L2 onboard clock and a retro-reflector array. These two components are used by T2L2 but are not integral to T2L2: the oscillator is the frequency reference of the DORIS System [11] and the LRA is used for satellite laser ranging (figure 2).

The photo detection device includes two avalanche photodiode photo detectors. One of them works in a nonlinear mode for time tagging purposes [12], the other works in a linear mode to trig the non linear detector and to measure the received laser energy. The most important function of the non-linear photo detector is to generate an electrical pulse from a very low level of light. The propagation delay inside the photo detector depends on the photon number. To avoid the temporal noise that would be introduced by an uncontrolled energy variation of the laser pulse (atmosphere, pointing error, laser variation and so on) this internal delay is compensated for. This is achieved with the linear photo detector giving the energy received. This energy together with the arrival time is recorded in real time onboard and downloaded to ground every two hours. The compensation for the internal delay of the detector is achieved by means of a post treatment process [13, 18]. The laser energy received at the satellite plane is sent to the photo-detectors through two distinct optics assemblies.
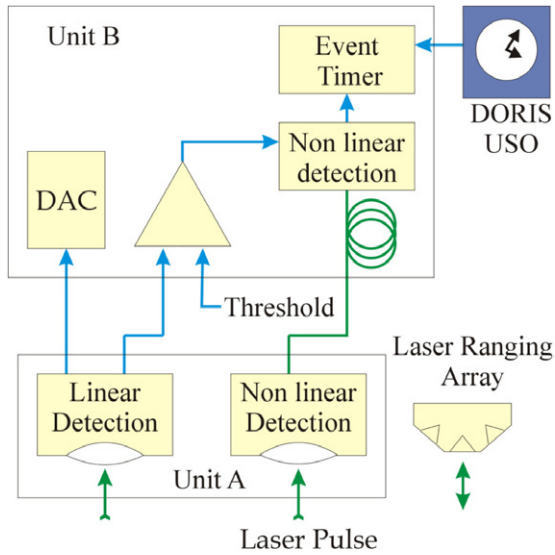
Figure 2. T2L2 Global architecture with unit A outside the satellite oriented toward the earth direction and unit B inside the payload. The DORIS USO and the LRA equipments are not a T2L2 subassembly.

This allows the geometry to fit the field of view of the instrument, the photon number to be adjusted and the spectral band width to be fixed. All this instrumentation is divided on the Jason 2 payload in two units A and B.

3. Ground to space time transfer

The offset Δ_{AS} between a ground clock A and the space clock S is given by:

$$\Delta_{AS} = \frac{t_E + t_R}{2} - t_B + \frac{C_{Sag}}{2} + C_{Rel} + C_{Atm} + C_{ICal} + C_{ECal} \quad (2)$$

where t_E and t_R are respectively the emission and reception epochs of laser pulses at the laser station, t_B the reception epoch on board, C_{Sag} a correction due to the speed aberration, C_{Rel} a term illustrating the relativistic frequency shift [13], C_{Atm} an atmospheric correction and C_{ICal} (internal calibration), C_{ECal} (external calibration) are two calibration terms to obtain respectively the time of flight between the reference point of the station and the satellite and the epoch of laser events at the reference point of the laser station. In order to minimize the noise associated with the measurement of the time of flight (computed from t_R and t_E in equation (2)), some reception epochs $t_{R'}$ are computed from an interpolation calculated on the actual measure t_R. This process also allows the use of laser events which have been detected on board the satellite but not on the ground. It is especially important for laser stations using a single photon mode detector (where the detection probability is in the range of 10%). In this case, the number of echoes detected by the laser station may be several times lower than the number of detected events on board.

C_{Sag} is associated with the computation of the time coordinates to take into account the propagation of laser pulses. C_{Sag} is given by:

Figure 3. STX301-002R SigmaTime sub-picosecond event timer designed for the calibration of laser stations.

Table 1. Main characteristics of the T2L2 calibration station.

Parameters	Values
Time stability @ 1000s (TDev)	< 20 fs
Linearity	0.3 ps RMS
Standard deviation	700 fs RMS
Optical input bandwidth	DC − 20 GHz
Electrical input bandwidth	DC − 8 GHz

$$C_{Sag} = \frac{2}{c^2}(x - X) \cdot \dot{X}. \quad (3)$$

It is computed from the coordinates x from the satellite and X from the station for each emission epoch.

C_{Rel} is associated with the transformation from the proper time of the onboard clock to coordinate time. It is a frequency shift of the space oscillator integrated as a function of time. C_{Rel} is given by:

$$C_{Rel} = \int \frac{1}{c^2}\left(\frac{\dot{x}^2}{2} - \frac{GM_E}{x}\right) dt \quad (4)$$

where GM_E is the geocentric gravitational constant. This relativistic frequency shift includes a constant term, which can be neglected in the ground to ground time transfer, and also a periodic term. The amplitude of the periodic frequency shift integrated over an orbit is in the range of 100 ps.

C_{Atm} is a correction reflecting the optical path difference introduced by the atmosphere between the uplink and the downlink. The worst case occurs with a laser station located near the equator and an observation of the satellite at a very low elevation angle (typically 5°). In that case, the time delay for the one-way link is roughly 40 ns and the time correction C_{Atm} between the uplink and the downlink is 1.5 ps.

C_{ICal} is obtained from epochs measured by means of laser pulses sent to the reception chain of the station by means of a calibration corner cube located in the laser beam (figure 1) at a set distance d_{cc} from the spatial reference of the station (cross axes of the telescope mount). This is measured at the same time as the acquisition of echoes on the satellite from the mean value of an ensemble of N_{ICal} epoch differences:

$$C_{ICal} = \left\langle t_E - t_{\widetilde{R}} \right\rangle_{N_{ICal}} - \delta_{cc}, \quad (5)$$

$t_{\widetilde{R}}$ being the reception epochs of laser pulses coming from the retro reflector and δ_{cc} a correction term taking into account the distance between the reference corner cube and the cross axis of the telescope.

C_{ECal} is measured by means of a dedicated calibration process. Laser stations are basically designed to measure the
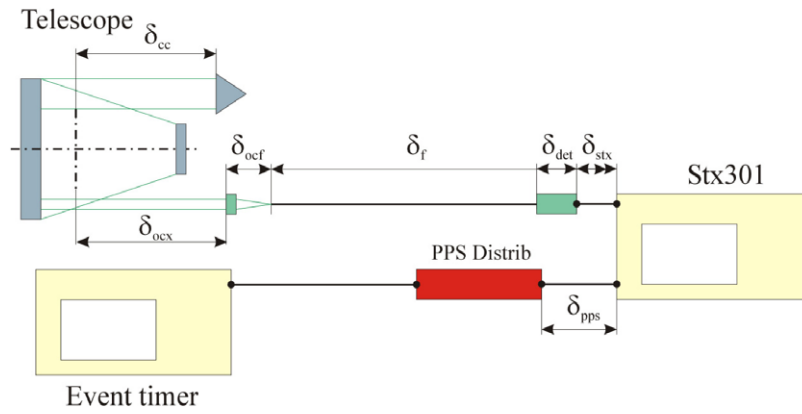
Figure 4. Definition of the propagation term through the telescope to the PPS distribution unit.
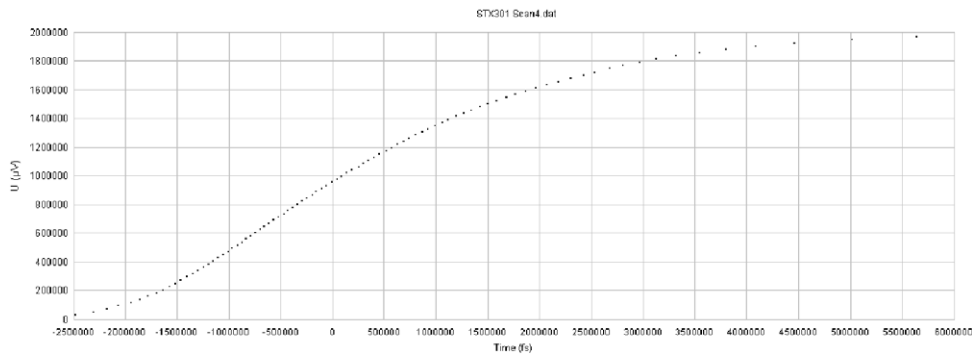

Figure 5. PPS Scan measured by the Sigma time STX301 event timer.

time difference between a start and a stop with an accuracy of the start pulse of typically 100 ns. In order to obtain the picosecond accuracy required for T2L2, laser stations are carefully calibrated with a dedicated calibration station. This calibration is based on a set of simultaneous measurements made of the habitual chronometry of the laser station and the dedicated calibration station. It permits measurement of the delay between the optical pulse at the cross axis of the telescope and the electrical reference coming from a given output of the PPS distribution unit of the time and frequency laboratory. The calibration station gathers all the metrology required to perform that measurement in a unique piece of equipment: this comprises a SigmaTime STX301 sub-pico-second event timer (figure 3), an optical module to grab laser pulses from the laser station and an optical fiber (figure 4). The event timer has two independent channels connected to optical and electrical inputs. The optical module comprises a collimation optic connected to a 50 m mono mode optical fiber (532 nm).

Characteristics of the calibration station are given in table 1.

The term C_{ECal} is computed from the mean value of an ensemble of N_{ECal} measurements. The time equation that allows the accurate time-tagging of laser pulses may be written as:

$$C_{\mathrm{ECal}} = \left\langle t_{\mathrm{E}} - t_{\widetilde{\mathrm{E}}e} \right\rangle_{N_{\mathrm{ECal}}} - \delta_{\mathrm{ocx}} + \delta_{\mathrm{PPS}} - (\delta_{\mathrm{ocf}} + \delta_f + \delta_{\mathrm{det}} + \delta_{\mathrm{stx}})$$

$$= \left\langle t_{\mathrm{E}} - t_{\widetilde{\mathrm{E}}} \right\rangle_{N_{\mathrm{ECal}}} - \delta_{\mathrm{ocx}} + \delta_{\mathrm{prg}}, \tag{6}$$

where $t_{\widetilde{\mathrm{E}}}$ is the emission epoch measured by the calibration station, δ_{ocx} the free space delay propagation between the station reference and the optical input of the calibration station, and δ_{prg} the global internal propagation inside the calibration station. δ_{PPS} is the delay in the PPS cable, δ_f the delay in the optical fiber, δ_{ocf} the delay of the collimation optic, δ_{det} the propagation constant induced by the optical to electrical conversion inside the detector [14] and δ_{stx} the delay in the cable between the detector and the event timer. By using the same calibration station to calibrate the different laser stations, the delays $\delta_{\mathrm{prg}} = \delta_{\mathrm{PPS}} - (\delta_{\mathrm{ocf}} + \delta_f + \delta_{\mathrm{det}} + \delta_{\mathrm{stx}})$ in equation (6) do not need to be known accurately. It must be emphasized that in this case, the calibration becomes relative since we do not know the real emission epoch of laser pulses. It is perfectly well suited for an accurate comparison of T2L2 with any other time transfer techniques from the temporal reference of each laboratory but it would become a difficulty if it was necessary to compare a given technique directly from the laser pulses.

The term $\left\langle t_{\mathrm{E}} - t_{\widetilde{\mathrm{E}}} \right\rangle$ is determined from the time setting of the SigmaTime STX301 event timer and from a simultaneous acquisition of an ensemble of laser pulses from the laser station and the calibration station. The time setting process allows the acquisition of measurements directly referenced to the time reference of the laboratory. It is carried out using a preliminary measurement of the PPS reference signal of the laboratory. The PPS threshold level is always set at 1 V. The time stability over one day of a typical PPS signal is in the range of 20 ps. To minimize the uncertainty of that time setting process, the PPS measurement is carried out over a set of $N_{\mathrm{TS}} = 30$ PPS

Table 2. Typical laser station.

Sub-system	Characteristics	Type	u/ps	Comments
Start detector	InGaAs pin photodiode, Band Width = 3 GHz Diameter 30 μm	A	5	Standard deviation obtained at constant threshold in a saturated mode [1, 22]
Return detector	Avalanche silicon photodiode, Geiger mode Diameter 200 μm	A	50	Standard deviation made in a single photon mode over the whole aperture [12, 14, 15]
Nd:YAG Laser	Active and passive mode locked laser, Flash pumped λ = 532 nm, 10 Hz, E = 50 mJ, FWHM = 100 ps	B	25	Uncertainty of the laser pulse width at half maximum (long and short term pulse variations)[4]
Event timer	2 independent channels, External frequency reference 10 MHz, Internal frequency PLL 200 MHz, resolution 1 ps	A	5	Standard deviation based on a perfect frequency reference [16, 21]
PPS Generator	Numerical division of a frequency source, 2.5 Vpp	A	20	Standard deviation of the output pulses as compared to the frequency reference [32]
TF lab to Laser Station cable	L < 100 m, Thermal $< \pm\ 5\,°C$, $<0.1\,\mathrm{ps\,K^{-1}\,m^{-1}}$	B	30	Uncertainty introduced by delay variations (thermal, radius, aging)[5]
Ref. Corner cube	Simple corner cube, localization ±1 mm	B	4	Uncertainty introduced by the geometrical measurement between the corner cube and the spatial reference of the station[6]

Table 3. Number of data considered for the uncertainty budget.

Number	Value
Emission N_E	1000
Reception N_R	300
On board N_B	200
PPS for time setting N_{TS}	30
Event of internal calib. N_{IC}	250
Event for external calib. N_{EC}	500

events. At the same time, a scan of that PPS signal is also performed by the event timer to determine the actual shape of the PPS signal. For that measurement, the event timer is used as an oscilloscope. It generates a graph where the abscissa axis is time and the ordinate axis is voltage. One channel of the event timer is used as the trigger for the time reference and the other is used to measure the signal. Figure 5 is an example of such a scan measured by the STX301 event timer.

4. Ground to ground time transfer

The ground to space time transfer computed from equation (2) can be used directly on individual echoes. It allows monitoring of the time transfer with the optimum temporal resolution (the typical time interval between consecutive laser event is roughly 1 s). The same computation, integrated over a few tens of seconds or over an entire satellite pass in order to minimize the white noise of the time transfer, is also of interest.

Ground to ground time transfer can be realized in either common-view or non-common-view mode. In the first case, the satellite is seen during a common period while in the other, the satellite is observed alternatively. For common-view, the maximum distance to the ground is roughly 6000 km.

Ground to ground time transfer depends very significantly on the visibility of the satellite. In common-view mode, the space oscillator is only solicited over the time interval of laser pulses (typically between 0.1 s to a few seconds). Over a longer period, noise is common for both stations and the difference vanishes. In the non–common-view mode, the noise of the space oscillator has to be considered over the time interval during which the satellite is not visible, and the noise of the space oscillator can become the main source of noise. That noise can be significantly reduced with a correction model C_{osc} taking into account parameters such as temperature, radiation or time. Up to now this model has not been operational. In what follows, we will only discuss ground to ground time transfer in common-view.

A ground to ground time transfer Δ_{AB} between two ground clocks A and B in common-view is computed from the difference between the individual time transfers x_{AS} and x_{BS} individually acquired by the stations. One has:

$$\Delta_{AB} = \Delta_{BS} - \Delta_{AS} + C_{osc}. \tag{7}$$

Since the laser emissions for each station are not synchronous, data from the ground to space time transfer of each station are first interpolated on the full seconds in the timescale of the satellite. The final time transfer x_{AB} is computed from the individual time transfer interpolated on the common full seconds.

5. Uncertainty budget

Considering that the terms of equation (2) are independent, the combined uncertainty of a time transfer $u_c(\Delta_{GS})$ between a ground clock and the space clock may be written as:

$$u_c^2(\Delta_{GS}) = \frac{u^2(t_E)}{4} + \frac{u^2(t_R)}{4} + u^2\left(t_B\right) + u^2(C_{ICal}) + u^2\left(C_{ECal}\right)$$
$$+ u^2(C_{Atm}) + \frac{u^2\left(C_{Sag}\right)}{4} + u^2(C_{Rel}). \tag{8}$$

---

[4] Streak camera measurements made on a Nd:YAG mode locked laser; laser rate: 10 ps, FWHM = 100 ps; passive mode locking (SESAM).

[5] Event timer measurement made on a coaxial cable having a length encountered in some typical laser stations (70 m).

[6] The corner cube is located at the output of the telescope; the reference of the station is materialized by the crossing of the axis of the telescope. The distance is classically done using a measuring tape.

Table 4. Emission epochs uncertainty $u(t_E)$.

Uncertainty Source	Type	u/ps	Observation
Laser station start detector time walk versus Laser FWHM	B	14	Induced by the duration fluctuations of laser pulses[7] [15]
Laser station start detector time walk versus laser energy	B	3	Induced by the energy variation of laser pulses[7] [20]
Laser station cable delay: laser to detector	B	6	Uncertainty introduced by delay variations of the coaxial cable used for the signal propagation (thermal)[5]
Laser station start detector internal noise	A	< 1	Standard deviation obtained at constant threshold in a saturated mode. The uncertainty is computed on the mean value over N_E [1, 22]
Frequency distrib. Between TF lab and laser station event timer	B	30	Uncertainty introduced by delay variations of the coaxial cable used for the distribution (thermal)[5]. The distribution is supposed free: no monitoring [32]
Time setting of the laser station event timer	A	4	Uncertainty computed on the over N_{TS}[8] [21]
Laser station event timer internal noise	A	< 1	Uncertainty computed on the mean value over N_E [21]
Combined uncertainty $u_c(t_E)$	A & B	34	Quadratic sum

Table 5. Reception epochs uncertainty $u(t_R)$.

Uncertainty source	Type	u/ps	Observation
Laser station return detector time walk versus laser FWHM	B	3	Induced by the duration fluctuations of laser pulses in a single photon detection mode[7] [12]
Laser station return detector time walk versus laser energy	B	5	Included by the energy variation of laser pulses in a single photon detection mode[7] [12, 22]
Laser station return detector time walk versus spot position	B	7	Speed aberration[9] [12]
Laser station return detector internal noise	A	3	Uncertainty computed on the mean value over N_R [12]
Laser station event timer internal noise	A	< 1	The uncertainty is computed on the mean value over N_R [21]
LRA signature	B	13	Attitude sensitivity[10] [23, 24]
False detection	A	4	White noise [20]
Atmosphere (uplink + downlink)	A	1	Uncertainty computed on the mean value over N_R [17]
Combined uncertainty $u_c(t_R)$	A & B	17	Quadratic sum

The combined uncertainty of a ground to ground time transfer in common view is given by:

$$u_c^2(\Delta_{AB}) = u_c^2(\Delta_{AS}) + u_c^2(\Delta_{BS}) + u^2(C_{osc}) \qquad (9)$$

Each uncertainty term in equations (8) and (9) is evaluated from other parameters. Some of them are evaluated using a statistical analysis of a series of observations (Type A) and others are arrived at using other methods (Type B).

Each uncertainty term should be determined on the basis of the precise experimental setup for a given link between two laser stations. In order to give a more general uncertainty budget, we will consider in the following a typical setup reflecting the characteristics of a large number of laser stations well suited for time transfer. The main uncertainties of such a station are summarized in table 2.

The final combined uncertainty depends also on the quantity of data acquired. Of this data, the number of laser events emitted N_E, echoes acquired N_R and events recorded on board N_B are especially important for the final uncertainty budget. The technical specifications of the laser station, together with observation conditions, of course have a strong influence on the outcome. For the sake of simplicity, these numbers are chosen to correspond to data acquired after a complete pass of the satellite above a ground station when observation conditions are difficult, with minimum on board events N_B equal to

200. For the MeO laser station, this requirement represents roughly 90% of recorded passes. This value ensures also a satisfactory signal to noise ratio. The number of measurements for the internal and external calibration process and time setting is selected so that there is a negligible uncertainty associated with the mean value of each of those terms. Table 3 gives the values for all these measurements.

5.1. Instrumental uncertainties $u(t_E)$, $u(t_R)$, $u(t_B)$, $u(C_{ICal})$, $u(C_{ECal})$

Regardless of the atmospheric correction C_{Atm} illustrating the difference between the up-link and the down-link, atmosphere has a significant role on the measurement of epoch t_B and t_R [17]. The air turbulence generates fluctuations of refractive index along the beam path which randomly modify the propagation delay. The turbulence can be characterized by the outer scale parameter L_o (size of the largest turbulent eddy), the

---

[7] The uncertainty is induced by the variations of the laser pulses (energy and pulse width) and the sensitivity of the start detector to these variations.
[8] The time setting of the event timer is done at the first initialization with the PPS reference of the Time and Frequency laboratory.
[9] The speed aberration of the satellite introduces an offset between the main axis of the reception channel and the line of sight. The uncertainty is introduced by this offset which generates a displacement of the laser spot on the detector and the sensitivity of the return detector to that displacement.

Table 6. On board epochs uncertainty $u(t_B)$.

Uncertainty source	Type	u/ps	Observation
Board detector time WALK versus laser FWHM	B	14	Induced by the duration fluctuations of laser pulses[7] [22, 24]
Board detector time walk versus laser energy	B	3	Included by the energy variation of laser pulses[7] [22, 24]
Board detector time walk versus incident angle	B	3	Optical path [24]
Board detector internal noise @ E_{Min}	A	5	Uncertainty computed on the mean value over N_B [24]
Board event timer internal noise	A	< 1	Uncertainty computed on the mean value over N_B [24]
LRA-detector geometry versus attitude	B	3	Attitude sensitivity[11] [24]
False detection on board	A	7	White noise [20]
Atmosphere (uplink)	A	< 1	Uncertainty computed on the mean value over N_B [17]
Combined uncertainty $u_c(t_B)$	A & B	16	Quadratic sum

Table 7. Internal calibration uncertainty $u(C_{ICal})$.

Uncertainty source	Type	u/ps	Observation
Laser station start detector time walk versus laser FWHM	B	14	Induced by the duration fluctuations of laser pulses[7] [15]
Laser station start detector time walk versus laser energy	B	3	Included by the energy variation of laser pulses[7] [20]
Laser station start detector internal noise	A	< 1	Standard deviation obtained at constant threshold in a saturated mode. Uncertainty computed on the mean value N_{IC} [1, 22]
Laser station event timer internal noise	A	< 1	Uncertainty computed on the mean value over N_{IC} [21]
Laser station return detector time walk versus laser FWHM	B	14	Induced by the duration fluctuations of laser pulses in a single photon detection mode[7] [12]
Laser station return detector time walk versus laser energy	B	3	Included by the energy variation of laser pulses in a single photon detection mode[7] [12, 22]
Laser station return detector time walk versus spot position	B	2	Center uncertainty[12]
Laser station return detector internal noise	A	3	Uncertainty computed on the mean value over N_{IC} [12]
Laser station event timer internal noise	A	< 1	Uncertainty computed on the mean value over N_{IC} [21]
False detection	A	1	White noise
Corner cube position of the laser station	B	4	Free space delay[6]
Combined uncertainty $u_c(C_{ICal})$	A & B	21	Quadratic sum

inner scale parameter L_i (size of the smallest eddy) and refractive index structure constant C_n (strength of turbulence). Up to now, the theoretical model of the atmospheric fluctuation does not accurately reflect the actual fluctuations measured by laser ranging. The most conservative measured value that can be used in the uncertainties of the two way laser ranging is 3 mm RMS [18]. This value implies an uncertainty on the up-link (t_B) of 5 ps (1.5 mm) and on the total link (t_R) of 10 ps (3 mm).

Tables 4–8 give an evaluation of the combined uncertainty of the whole instrumentation of the T2L2 Time transfer [19–22]. Each parameter $u(t_E)$, $u(t_R)$, $u(t_B)$, $u(C_{ICal})$ and $u(C_{ECal})$ is a combined uncertainty computed from the quadratic sum of other uncertainties depending on the instrumentation [23–25]. Tables 7 and 8 are divided in three sub-sections separated by double lines. The first sub-section shows uncertainties which are not specific to the calibration process: the instrumentation of the laser station is used under exactly the same conditions as those for a classical observation. The next sub-section shows uncertainties corresponding to measurements of events which are specific to the calibration process. The final sub-section is specifically related to the calibration equipment.

5.2. Atmospheric uncertainty $u(C_{Atm})$

The amplitude of the atmospheric correction C_{Atm} (difference between the up-link and the down-link) is 1.5 ps. The corresponding uncertainty $u(C_{atm})$ of that correction is in the fs domain and can be set to 0 in the framework of this study.

5.3. Sagnac and relativity uncertainties $u(C_{Sag})$, $u(C_{Rel})$

Both corrections C_{Sag} and C_{Rel} are calculated from the Jason 2 ephemerides and from the ITRF 2008 solution giving

[10] The reflected pulses are affected by a specific time signature coming from the superposition of the pulses reflected by each individual corner cube of the whole LRA. The uncertainty is introduced by this signature and the sensitivity of the return detector to the temporal shape of the laser pulse.
[11] Because the LRA and the detection unit are not located in the same place, the reflection and detection points do not coincide. The uncertainty is introduced by the accuracy location of both the LRA and the detection unit of the space instrument and by the attitude uncertainty of the Jason 2 satellite.
[12] The spot projected on the detector coming from the calibration does not have exactly the same shape nor the same position as those coming from the satellite. The uncertainty is introduced by these differences and the sensitivity of the return detector.

Table 8. External calibration uncertainty $u(C_{ECal})$.

Uncertainty source	Type	u/ps	Observation
Laser station start detector time walk versus laser FWHM	B	14	Induced by the duration fluctuations of laser pulses[7] [15]
Laser station start detector time walk versus laser energy	B	3	Included by the energy variation of laser pulses[7] [20]
Cable delay: laser to laser station start detector	B	6	Uncertainty introduced by delay variations of the coaxial cable used for the signal propagation (thermal)[5]
Laser station start detector internal noise	A	< 1	Standard deviation obtained at constant threshold in a saturated mode. Uncertainty computed on the mean value N_E [1, 22]
Time distribution between TF lab and laser station event timer	A	30	Uncertainty introduced by delay variations of the coaxial cable used for the distribution (thermal)[5]. The distribution is supposed free: no monitoring [32]
Time setting of the laser station event timer	A	4	Uncertainty computed on the over N_{TS}[8] [21],
Laser station event timer internal noise	A	< 1	Uncertainty computed on the mean value over N_E [21]
Calibration station start detector time walk versus laser FWHM	B	6	Induced by the duration fluctuations of laser pulses[13] [31]
Calibration station start detector time walk versus laser energy	B	6	Included by the energy variation of laser pulses[13] [31]
Calibration station Start detector internal noise	A	< 1	Uncertainty computed over the mean value over N_{EC}[13]
Time setting of the calibration station event timer	A	< 1	Uncertainty computed over the mean value over N_{TS}
Calibration station event timer internal noise	A	< 1	Uncertainty computed over the mean value over N_{EC}
Calibration station fiber delay: optic to detector	B	9	Thermal variation and aging [25]
Calibration station cable delay: ref. to event timer	B	2	BNC Connection[14]
Calibration station ref. optic position	B	4	Free space delay[15]
Combined uncertainty $u_c(C_{ECal})$	A & B	36	Quadratic sum

Table 9. Sagnac and relativity uncertainties $u(C_{Sag})$, $u(C_{Rel})$.

Uncertainty source	Type	u/ps	Observation
Combined uncertainty $u_c(C_{Sag})$	B	< 1	Negligible
Combined uncertainty $u_c(C_{Rel})$	B	< 1	Negligible

Table 10. Ground to space and ground to ground expanded uncertainties for a coverage factor = 2.

Time transfer	Type	u/ps	Comments
Ground to space expanded uncertainty $u_E(\Delta_{GS})$	A & B	98	$k = 2$
Ground to ground expanded uncertainty $u_E(\Delta_{GG})$	A & B	138	$k = 2$, Common view

station coordinates [26, 27]. The coordinate uncertainties of both the laser station and the satellite are in the range of a few centimeters leading to negligible uncertainties for those terms (table 9) [13]:

5.4. Ground to space and ground to ground extension of uncertainties $u_E(\Delta_{GS})$, $u_E(\Delta_{GG})$

The Ground to Space and the Ground to Ground uncertainties are computed from equations (8) and (9) with a number of acquired events given in table 3 (typically acquired during a single pass of the satellite). In the common-view mode, since the space oscillator is only solicited over the time interval between laser pulses, the uncertainty $u(C_{osc})$ may be neglected in comparison with the other noises.

In accordance with the recommendations given by the European Association of National Metrology Institutes (EURAMET), these uncertainties are computed for a coverage factor $k = 2$ [28]. The final uncertainty budget of the whole experience is summarized in table 10.

6. Validation

Observatoire de la Côte d'Azur (OCA) has two laser stations on the same site (MeO and FTLRS) that can be used together to realize a time transfer in a co-location configuration (figure 6). MeO is one of the biggest laser stations in the world with a 1.54 m telescope and a frequency doubled Nd:YAG laser (rate = 10 Hz, FWHM = 150 ps, Energy = 100 mJ) [29]. FTLRS is a

[13] The uncertainty is induced by the variations of the laser pulses (energy and pulse width) and the sensitivity of the calibration detector to these variations. The calibration detector is an ultrafast PIN photodiode having a bandwidth of 20 GHz and an impulse response of 18 ps (FWHM).
[14] Most of the connections used in the calibration setup are made with SMA connectors but the final connection with the main PPS distribution unit of the time and frequency laboratory is usually BNC. The mechanical reference uncertainty of BNC connector is better than 1 mm.
[15] The optical module of the calibration station is attached to the structure of the telescope, usually close to the secondary mirror of the instrument. The distance between the calibration module and the cross axis of the telescope is done with a measuring tape.
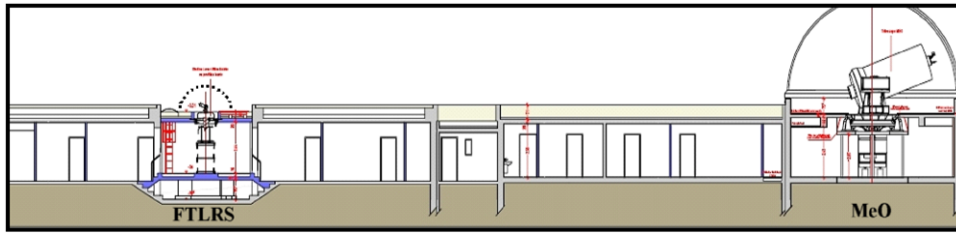
Figure 6. Laser stations at OCA. MeO: 1.54 m telescope; Nd:YAG laser @ 532 nm; rate = 10 Hz; FWHM = 150 ps; Energy = 100 mJ. FTLRS: 0.13 m telescope; Nd:YAG laser @ 532 nm; rate = 10 Hz; FWHM = 35 ps; Energy = 30 mJ.

Table 11. Ground to space and ground to ground expanded uncertainties with an active monitoring of the cable connecting T&F Lab and Laser station for a coverage factor = 2.

Time transfer	Type	u/ps	Comments
Ground to space expanded uncertainty $u_E(\Delta_{GS})$	A & B	55	$k = 2$
Ground to ground expanded uncertainty $u_E(\Delta_{GG})$	A & B	77	$k = 2$, Common view

transportable system using a very small telescope (13 cm) and also a doubled frequency Nd:YAG laser (rate = 10 Hz, FWHM = 35 ps, Energy = 30 mJ) [30]. The distance between the two SLR stations is 35 m.

Since the beginning of the T2L2 mission on Jason 2, five co-location experiments have been made at OCA. Among them, one was conducted in spring 2010, with a unique H-Maser connected to both MeO and FTLRS [31]. Another was performed between March and April 2012 with two independent clocks connected to FTLRS (Caesium) and to MeO (H-Maser) and also two independent GPS receivers (Dicom GTR50) and an ultra stable event timer (STX301) to intercompare T2L2 results with GPS and direct comparison [32].

In the first experiment made with a unique clock for both MeO and FTLRS, the comparison is made directly based on the differences between calibration and T2L2 results. One gets from nine common passes acquired in four days (filtered @ ± 3σ):

$$\Delta_{Meo.FTLRS} = 37 \text{ ps} \tag{10}$$

$$u(\Delta_{Meo.FTLRS}) = 60 \text{ ps}; \ k = 1. \tag{11}$$

This result is in close agreement with the uncertainty budget given in table 10.

For the second experiment, conducted with an independent clock for each station, a comparison was made between the calibrated T2L2 link (MeO-FTLRS) and a direct comparison was based on the STX301 event timer. The computation took into account the important drift existing between the caesium and the H-Maser in order to avoid any error in the epochs of realization of each comparison. The global uncertainty budget of the comparison depends on the uncertainties of the ground to ground time transfer and also on the uncertainties introduced by the direct comparison. It includes uncertainties in cables, output to output skew introduced by pulse distribution units and errors generated by the interpolation process. The combined uncertainty of that direct comparison is estimated

at $u_c(\Delta_{Direct}) = 50$ ps [33], giving an extend uncertainty of $u_E(\Delta_{Direct}) = 100$ ps with a coverage factor of 2. One gets for a given pass:

$$\text{T2L2}: \Delta_{Meo.FTLRS} = 95\,910 \text{ ps} \tag{12}$$

$$\text{STX30 1}: \Delta_{Meo.FTLRS} = 96\,076 \text{ ps}. \tag{13}$$

The difference between T2L2 and direct comparison is 166 ps which is compatible with the quadratic sum of $u_E(\Delta_{GG})$ given in table 10 and $u_E(\Delta_{Direct})$.

7. Perspectives and conclusions

In the typical laser station summarized in table 2, the most significant uncertainty terms come from the delay variation (thermal) of the cable between the time and frequency laboratory and the event timer of the laser station and from the laser pulse width variation. To improve the former, we designed an ultra stable time signal generator including an event timer able to monitor the time delay variation in the propagation of the signals (SigmaTime STS201) [32]. This monitoring is performed by means of a double propagation of the signal emitted by the distributor and repeated by the user (laser station). The overall standard deviation of the instrument (distribution and monitoring) is better than 1.5 ps RMS. With such a performance and with a laser having a pulse width uncertainty of 10 ps, the ground to ground expanded uncertainty becomes smaller than 100 ps (table 11).

Another way to improve the global uncertainty of T2L2 is to improve our knowledge of the duration of the laser pulses emitted by the laser station. Up to now, the pulse width has been determined using a dedicated process performed by the calibration station using high speed photo detection triggered alternatively from positive to negative slope. This process is perfectly well suited to our needs but requires good laser energy stability. Some pulse widths in the range of 20 ps were measured using this process. When the energy stability is not high enough, the measurement can be biased by a significant factor. In this case a single photon measurement may be preferable. The pulse width is determined from data acquired by a dual channel event timer triggered by a multi photo detector and stopped by a single photon detector. This process would permit the use of a single photon detector as a detection device, permitting the simultaneous measurement of pulse width and time delay. This single photon detector has been built and will be used in the next calibration process [34].

Today, the T2L2 experiment launched in 2008 on the satellite Jason 2 is fully operational. It gives a unique opportunity to perform time transfers in common-view between remote sites with an uncertainty better than 140 ps (coverage factor = 2). It allows accurate comparisons with other microwave time transfer systems using a totally independent technique. Some direct comparisons of collocated observations and other dedicated experiments have also enabled us to validate the uncertainty budget described in section 5.

The T2L2 space mission has been extended until 2017. This extension will allow for non-common-view time transfer realization, link budget analysis and other optical time transfer comparisons [35]. If the timetable is compatible with the launch of the ACES mission, some time transfer comparisons between the optical time transfer of ACES (European Laser Timing ELT) and T2L2 should be scheduled at the mission start-up together with some comparisons with the microwave link MWL also embedded on ACES.

Acknowledgment

References

[1] Fridelance P, Samain E and Veillet C 1997 T2L2—time transfer by laser link: a new optical time transfer generation *Exp. Astron.* **7** 191–207

[2] Samain E, Weick J and Vrancken P 2008 Time transfer by laser link—the T2L2 experiment on JASON-2 and further experiments *Int. J. Mod. Phys.* D **17** 1043–54

[3] Guillemot P, Samain E, Vrancken P, Exertier P and Leon S 2008 Time transfer by laser link—T2L2: an opportunity to calibrate RF links *Proc. PTTI* pp 95–106

[4] Rovera G D *et al* 2014 A direct comparison between two independently calibrated time transfer techniques: T2L2 and GPS common-views *Proc. CPEM* (*Rio de Janeiro*) pp 666–7

[5] Samain E *et al* 2014 A sub-ns comparison between GPS common view and T2L2 *Proc. EFTF* (*Neuchatel, Switzerland*)

[6] Cacciapuoti L and Salomon C 2011 Atomic clock ensemble in space *J. Phys.: Conf. Ser.* **327** 012049

[7] Wolf P and Petit G 1997 Satellite test of special relativity using the global positioning system *Phys. Rev.* A **56** 4405

[8] Samain E 2002 One way laser ranging in the solar system. The TIPO Project (Telemetrie lnterPlanetaire Optique) *Proc. EGS XXVII General Assembly Heft Nr.* (*Nice, France, 2004*) vol 69 pp 80–5

[9] Veillet C 1993 SORT: Solar Orbit Relativity Test, a proposal in the discipline area of fundamental physics in response to ESA's call for mission concepts for the follow-up to horizon 2000

[10] Degnan J J, Smith D E and Turcotte D L (ed) 1993 Millimeter accuracy satellite laser ranging: a review *AGU Geodyn. Ser.* **25** 133

[11] Auriol A and Tourain C 2010 DORIS system: the new age *Adv. Space Res.* **46** 1484–96

[12] Samain E 1998 Timing of optical pulses by photodiode in Geiger mode *Appl. Opt.* **37** 502–6

[13] Exertier P, Samain E, Martin N, Courde C, Laas-Bourez M, Foussard C and Guillemot P 2014 Time transfer by laser link: data analysis and validation to the ps level *Adv. Space Res.* **54** 2371–85

[14] Prochazka I, Blazej J and Kodet J 2011 Measurement of the optical to electrical detection delay in the detector for ground-to-space laser time transfer *Metrologia* **48** L13–6

[15] Villa F *et al* 2014 CMOS SPADs with up to 500 μm diameter and 55% detection efficiency at 420 nm *J. Mod. Opt.* **61** 102–15

[16] Samain E 1995 Le laser lune Millimétrique et Nouvelles méthodes de datation optique *PhD Dissertation* Université de Nice Sophia Antipolis

[17] Prochazka I and Kral L 2002 Atmospheric contribution to the laser ranging Jitter *Proc. 13th Int. Laser Ranging Workshop* (*Washington, DC, 2002*)

[18] Mulacova J *et al* 2004 Effects of the atmosphere on the SLR precision *Proc. 14th Int. Laser Ranging Workshop*

[19] Samain E *et al* 1998 Millimetric lunar laser ranging at OCA *Astron. Astrophys. Suppl. Ser.* **130** 235–44

[20] Samain E Fridelance P and Guillemot P 2010 An ultra-stable event timer designed for T2L2 *Proc. EFTF* (*Noordwijk, Netherlands*)

[21] Vrancken P 2008 Characterization of T2L2 (time transfer by laser link) on the Jason 2 Ocean altimetry satellite and micrometric laser ranging *PhD Dissertation* Université de Nice—Sophia Antipolis

[22] Arnold D A 2002 Retro-reflector array transfer functions *Proc. 13th Int. Laser Ranging Workshop* (*Washington, DC*)

[23] Weick J *et al* 2007 Prospective performance budget of the T2L2 experiment *Proc. Frequency Control Symp.* pp 312–4

[24] Samain E *et al* 2014 Time transfer by laser link (T2L2): characterization and calibration of the flight instrument *Metrologia* **51** 503

[25] Kuznetsov M *et al* 2013 Electronic and thermal refractive index changes in Ytterbium-doped fiber amplifiers *Optic Express* **21** 22374–88

[26] Cerri L *et al* 2010 Precision orbit determination standards for the Jason series of altimeter missions *Marine Geod.* **33** 379–418

[27] Altamimi Z *et al* 2011 ITRF2008, an improved solution of the international terrestrial reference frame *J. Geod.* **85** 457–73

[28] BIPM 2008 Evaluation of measurement data—guide to the expression of uncertainty in measurement JCGM 100:2008

[29] Samain E *et al* 2008 MeO: the new French lunar laser station *Proc. 16th Int. Laser Ranging Workshop* (*Poznan, Poland*)

[30] Nicolas J *et al* 2001 Centimeter accuracy for the French transportable laser ranging station (FTLRS) through sub-system controls *Surv. GeoPhys.* **22** 449–64

[31] Samain E *et al* 2011 Time transfer by laser link—T2L2: current status and future experiments *Proc. Frequency Control and the European Frequency and Time Forum*

[32] Samain E *et al* 2012 T2L2: ground to ground time transfer *Proc. EFTF* pp 36–40

[33] Laas-Bourez M *et al* 2014 Accuracy validation of T2L2 time transfer in co-location *IEEE Trans. Ultrason. Ferroelectr. Freq. Control* **62** 255–65

[34] Samain E *et al* 2013 Time transfer by laser link—T2L2: microwave link comparison *Proc. of the 18th Int. Laser Ranging Workshop*

[35] Schreiber U *et al* 2009 The European laser timing (ELT) experiment on-board ACES *Proc. of Frequency Control and the European Frequency and Time Forum*